

# Exchange Flow Rate Measurement Technique in Density Different Gases

**Motoo FUMIZAWA**

ME Dept., Shonan Institute of Technology, Fujisawa, 251-8511 Japan

**Shuhei OHKAWA, Isaku BUMA and Suguru TANAKA**

Graduate School of ME Shonan Institute of Technology, Fujisawa, 251-8511 Japan

## ABSTRACT

Buoyancy-driven exchange flows of helium-air through inclined a narrow tube was investigated. Exchange flows may occur following the opening of a window for ventilation, as well as when a pipe ruptures in a high temperature gas-cooled reactor. The experiment in this paper was carried out in a test chamber filled with helium and the flow was visualized using the smoke wire method. A high-speed camera recorded the flow behavior. The image of the flow was transferred to digital data, and the slow flow velocity, i.e. micro flow rate was measured by PIV software. Numerical simulation was carried out by the code of moving particle method with Lagrange method.

**keywords:** Buoyancy, Exchange flow, Helium, Smoke wire, PTV, Densimetric Froude number, HSMAC-method, Numerical analysis moving particle method, Lagrange method

## 1. INTRODUCTION

Buoyancy-driven exchange flows of helium-air were investigated through horizontal and inclined small openings. Exchange flows may occur following the opening of a window for ventilation, the outbreak of fire in a room or over an escalator in an underground shopping center, as well as when a pipe ruptures in a modular high temperature gas-cooled nuclear reactor. The fuel loading pipe is located in an inclined position in

a pebble bed reactor such as the Modular reactor [1, 2] and AVR [3, 4].

In safety studies of High Temperature Gas-Cooled Reactor (HTGR), the failure of a standpipe at the top of the reactor vessel or a fuel loading pipe may be one of the most critical design-based accidents. Once the pipe ruptures, helium immediately rushes up through the breach. Once the pressure between the inside and outside of the pressure vessel has balanced, helium flows upward and air flows downward through the breach into the pressure vessel. This means that buoyancy-driven exchange flow occurs through the breach, caused by the density difference of the gases in the unstably stratified field. Since an air stream corrodes graphite structures in the reactor, it is important to evaluate and reduce the air ingress flow rate when a standpipe rupture occurs. To date, studies have been performed on the exchange flow of two fluids with different densities through vertical and inclined short tubes. Epstein [5] studied the exchange flow of water and brine through various vertical tubes, experimentally and theoretically. Mercer et al.[6] experimentally studied an exchange flow through inclined tubes with water and brine. The latter experiments were carried out in the range of  $3.5 < L/D < 18$  and  $0 \text{ deg} < \theta < 90 \text{ deg}$ , and indicated that the length-to-diameter ratio  $L/D$ , and the inclination angle  $\theta$  of the tube are the important parameters for the exchange flow rate.

Most of these studies were performed on the exchange flow using a relatively small difference in the densities of the two fluids (up to 10 per cent). However, in the case of a HTGR standpipe rupture, the density of the outside gas is at least three times larger than that of the gas inside the pressure vessel. Few studies have been performed so far using such a large density difference. Kang et al.[7] studied experimentally the exchange flow through a round tube with a partition plate. Although one may assume that the partitioned plate, a kind of obstacle in the tube, would reduce the exchange flow rate, Kang found that the exchange flow rate was increased by the partition plate because of separation of the upward and downward flows.

The objectives of the present study are to investigate the behavior of the exchange flow, then to evaluate the exchange flow rate using the PTV and PIV methods, as well as mass increment with the helium-air system. The following methods are applied the present study.

- (1) numerical analysis
- (2) smoke wire method (SW)
- (3) mass increment method (MI)
- (4) optical system of the Mach-Zehnder interferometer

## 2. NUMERICAL ANALYSIS

Two dimensional unsteady code of HSMAC method is adopted to the buoyancy-driven exchange flow system [1]. In the code, thermal hydraulic program is described basic equation of mass, momentum and energy. The energy equation is transferred to mass diffusion equation, as shown in Figure 1. Analysis coordinate is shown in Figure 2. The left part is test chamber filled with helium gas and the right part is outside region filled with air. Typical calculation result is shown in Figure 3, where is the narrow channel, between the left and right. The exchange flow occurs with vortex in the narrow channel. Therefore, the center flow rate  $Q_1$  is larger than the right edge flow rate  $Q_2$ , as shown in Figure 4.

Conversion from energy eq. (temperature) to mass diffusion

Mass eq.  $\frac{\partial v_x}{\partial x} + \frac{\partial v_y}{\partial y} = 0$

Momentum eq.

Energy eq.  $\rho c_p \left( \frac{\partial T}{\partial t} + v_x \frac{\partial T}{\partial x} + v_y \frac{\partial T}{\partial y} \right) = \lambda \left( \frac{\partial^2 T}{\partial x^2} + \frac{\partial^2 T}{\partial y^2} \right)$

unsteady

convection

thermal conductivity

Temperature  $T \rightarrow$  mass fraction  $\omega_A$  as A element

$\frac{\lambda}{\rho c_p} \rightarrow$  diffusion coefficient  $D_{AB}$  as A,B element

Mass diffusion eq. of He as A element  $\left( \frac{\partial \omega_A}{\partial t} + v_x \frac{\partial \omega_A}{\partial x} + v_y \frac{\partial \omega_A}{\partial y} \right) = D_{AB} \left( \frac{\partial^2 \omega_A}{\partial x^2} + \frac{\partial^2 \omega_A}{\partial y^2} \right)$

unsteady

transfer

diffusion

Fig.1 Basic equations of energy and mass diffusion

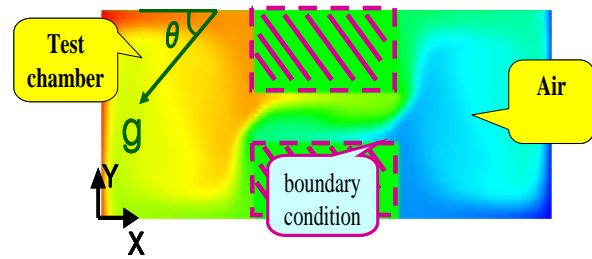


Fig.2 Analytical coordinate and conditions

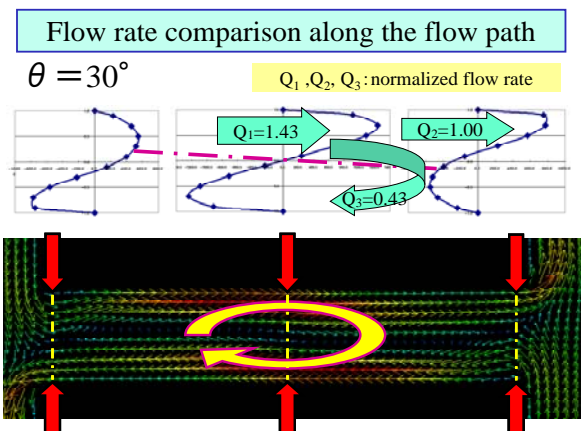
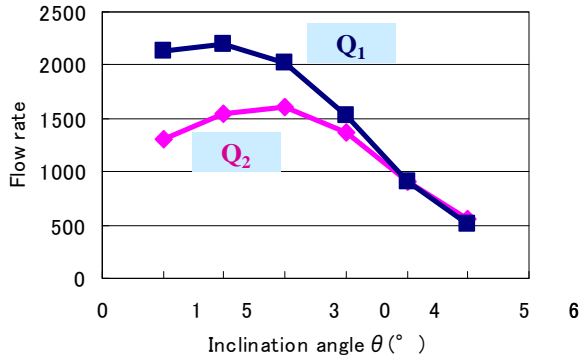


Fig.3 Analytical result of narrow flow path of Exchange flow



The Flow rate  $Q_1$  is higher than  $Q_2$

Fig.4 Relation of Exchange flow rate and inclination angle of analytical results

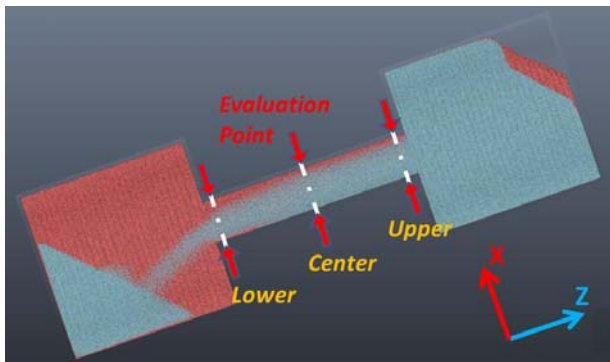


Fig.5 Flow velocity distribution on XZ cross section

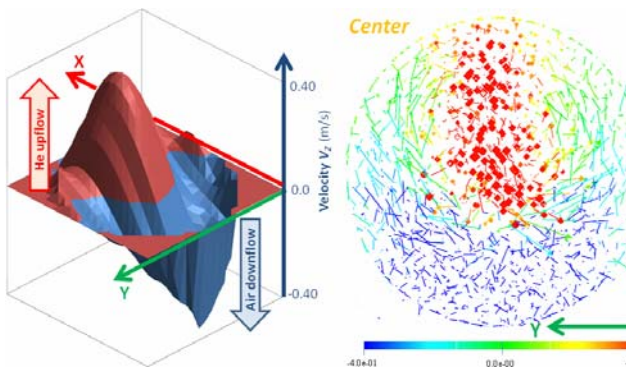


Fig.6 Bird eye view of main flow velocity distribution and secondary flow velocity distribution on XY section on the center plain of XY co-ordinate

Another numerical simulation was carried out by the code of moving particle method with Lagrange method. Figure 5 shows the flow velocity distribution on XZ cross section. Figure 6 Bird eye view of main flow velocity distribution and secondary flow velocity distribution. In the figures, the Counter flow was observed and also the vortex pair was clearly shown in the narrow pipe.

### 3. SMOKE WIRE MWTTHOD

#### 3.1 Experimental apparatus and procedure

The smoke wire method (SW) was used for the present investigation. Figure 7 shows a typical sketch of the apparatus. It consists of a smoke pulse generator, a thin Nichrome wire coated with oil and a test chamber. This figure also shows the high-speed camera system, which transfers the visual digital data to the personal computer for data acquisition. The experimental procedure is as follows. The test chamber is filled with pure helium. By removing the cover plate placed on the top of the tube, the exchange flow is initiated. Under such conditions, the smoke pulse generator ignites the high voltage. Immediately smoke appears and the helium up flow and air down flow are visualized in the flow path of the long tube. The high-speed camera system records the visual data up to 1600 frames per second. The upward flows peak velocity is measured by PTV and PIV method.

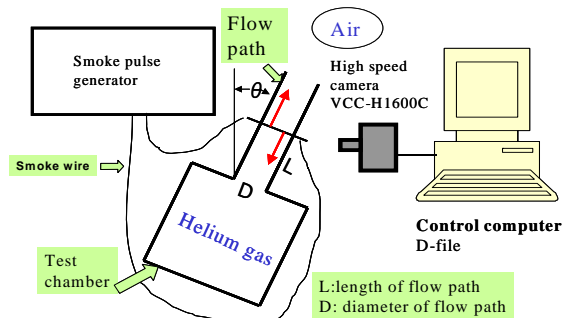


Fig.7 Exchange flow apparatus of smoke wire method high speed camera system

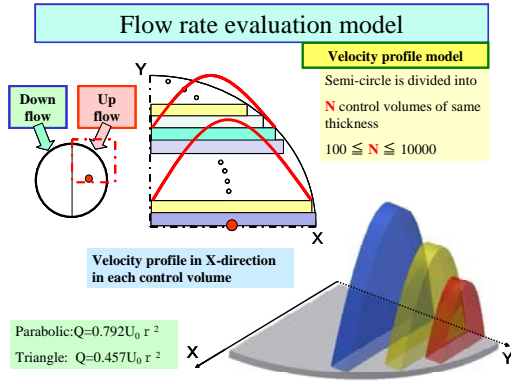


Fig.8 Flow rate evaluation model in smoke wire method

### 3.2. Results

The typical exchange flow in the tube was visualized. The visualized exchange flow resembles an S-shape. The frames are set at 200 and 500 frames per second in the high-speed camera. The visualized data is listed along the elapsed time, the upward flow peak velocity measured by PTV. In the case of  $L/d=10$ , the average velocity value  $U_0$  is evaluated as 0.662 m/s. This signifies that high exchange velocity is detected in a low  $L/D$  ratio. Assuming flow model of a parabolic flow profile, as shown in Figure 8, the exchange flow rate  $Q$  is derived as follows, where  $r$  is the radius of the flow path in a horizontal direction. Result is shown in Figure 9. The flow rate  $Q$  is the highest in the 30 degree.

$$Q = 0.792 U_0^2 \quad (1)$$

The densimetric Froude number is defined by the following equation derived from the dimensional analysis suggested by Keulegan [8]:

$$Fr = \frac{Q}{A} \sqrt{\frac{\rho}{gD \Delta \rho}} \quad (2)$$

In the PTV method, the exchange flow rate  $Q$  is calculated as  $1.47 \times 10^{-5} \text{ m}^3/\text{s}$  under the condition

of  $L/D=10$ . Therefore, the densimetric Froude number  $Fr$  is evaluated as 0.202, and in this condition Reynolds number  $Re$  is 79.2. When  $L/D=10$ , the densimetric Froude number  $Fr$  is evaluated as 0.287.

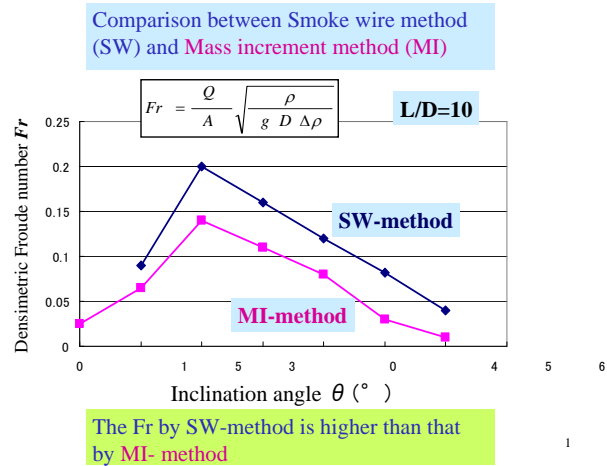


Fig.9 Relation of Densimetric Froude number and inclination angle in both experiments

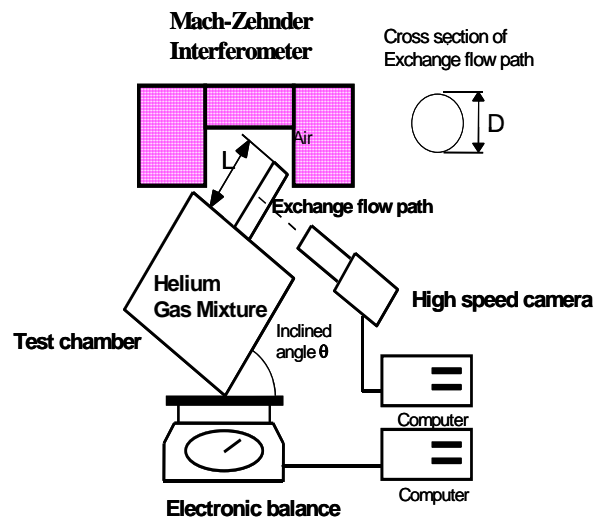


Fig.10 Experimental apparatus of optical system and mass increment

## 4. METHOD OF MASS INCREMENT

### 4.1 Experimental apparatus and procedure

The mass increment method (MI) was used for the investigations. Figure 10 shows a rough sketch of the apparatus. It consists of a test chamber, an electronic balance and a personal computer for data acquisition. The experimental procedure is mentioned in Sec. 2.1. Air enters the test chamber and the mass of the gas mixture in the test chamber increases. The mass increment  $\Delta m$  is automatically measured by the high accurate electronic balance. The density increment of the gas mixture  $\Delta \rho_L = \Delta m/V$  is calculated from mass increment data. The density increment signifies the difference between densities of the gas mixture from the density of pure helium in the test chamber. Subsequently, the volumetric exchange flow rate is evaluated using the following equation:

$$Q = \frac{V}{\rho_H - \rho_L} \cdot \frac{d(\Delta \rho_L)}{dt} \quad (3)$$

In the above equations,  $V$  is the volume of the test chamber,  $\rho_H$  the density of air,  $\rho_L$  the density of the gas mixture in the test chamber,  $\Delta \rho_L (= \rho_H - \rho_{He})$  = the density increment of the gas mixture,  $t$  the elapsed time,  $U(=Q/A)$  the exchange-velocity,  $\rho (= \rho_H + \rho_{He})/2$ ,  $D$  the diameter and  $g$  the acceleration of gravity. The experiments are performed under atmospheric pressure and room temperature using the vertical and inclined round tubes, and using a vertical annular tube. The density of the gas mixture is close to that of helium in the present experiment. The sizes of the tubes are as follows. The diameter of the round tube  $D$  is 20 mm, which is much smaller than that of the test chamber. The inclination angle  $\theta$  ranges from 15 to 90 deg and the height  $L$  ranges from 0.5 to 200 mm.

### 4.2. Results and discussion

It is already known that the densimetric Froude number is regarded as constant within a time

duration when the gas in the upward flow is assumed to be helium [10]. Figure 8 shows the relationship between  $Fr$  and inclination angle  $\theta$  with  $L/D$  as a parameter. For inclined tubes,  $Fr$  is larger than that for vertical tubes. The black circles show the experimental data for the orifice (i.e.  $L/D = 0.05$ ) and the black rhombuses for the long tube (i.e.  $L/D = 5$ ). The densimetric Froude number reaches the maximum at 60 deg for the orifice and 30 deg for the long tube. It is found that the angle for the maximum  $Fr$  decreases with the increase of  $L/D$  in the helium-air system.

## 5. OPTICAL SYSTEM OF MACH-ZEHNDER INTERFEROMETER

### 5.1 Experimental apparatus and procedure

The optical system of the Mach-Zehnder interferometer, MZC-60S to visualize the exchange flow is shown in Figure 10. After being rejoined behind the splitter, the test and reference laser beams interfere, and the pattern of interference fringe appears on the screen. If the density of the test section is homogeneous, the interference fringes are parallel and equidistant [9]. If the density is not homogeneous, the interference fringes are curved. Inhomogeneity in the test section produces a certain disturbance of the non-flow fringe pattern. The digital camera and high-speed camera using a D-file can be attached to the interferometer.

### 5.2. Results

Figure 11 shows the typical interference fringes for an inclined long tube ( $L/D=5$ ). The curved interference fringes indicate that the lighter helium flows in the upper passage of the tube. The straight fringes indicate that the heavier air flows in the bottom of the tube. It is clearly visualized that the exchange flows take place smoothly and in a stable manner in the separated passages of the tube. This leads to less resistance for the exchange flow in the inclined tubes compared to the vertical ones. In the case of a 30

deg. angle, the curvature of the interference fringes is larger than that at other angles, indicating that the exchange flow rate and the densimetric Froude number are the largest at 30 deg.

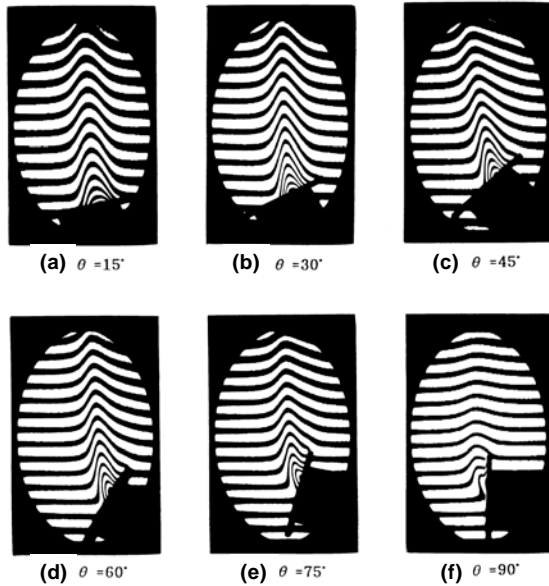


Fig.11 Typical interference fringes for an inclined long round tube ( $L/D=5$ )

## 6. CONCLUSION

- (1) Flow visualization results indicate that the exchange flows through the inclined round tube take place smoothly and in a stable manner in the separated passages of the tube.
- (2) Assuming velocity profile, exchange flow rate ,i.e., densimetric Froude number are evaluated.
- (3) Densimetric Froude number  $Fr$  by SW-method is higher than that by MI- method.
- (4) Numerical calculation predicts the circulation flow occurs in the narrow flow path.

## ACKNOWLEDGEMENTS

The authors are deeply indebted to Dr. Makoto Hishida, professor of Chiba University in Japan,

for his unfailing interest and helpful input to this study.

## 7. REFERENCES

- [1] Fumizawa,M. ; **Proc. HT2005 ASME Summer Heat Transfer Conference**, HT2005-72131, Track 1-7-1 (2005) , pp.1-7.
- [2] Kiso et.al.;**JSME Annual MTG**, (1999) pp.339-340.
- [3] M.M.El-Wakil, **Nuclear Energy Conversion**, Thomas Y. Crowell Company Inc., USA (1982)
- [4] Arbeitsgemeinschaft Versuchs-Reactor AVR, "Sicherheitsbericht fuer das Atom -Versuchskraftwerk „Juelich" (1965)
- [5] Epstein,M., **Trans. ASME J. Heat Transfer**, 110, (1988) ,pp.885 -893
- [6] Mercer, A. and Thompson.H., **J. Br. Nucl. Energy Soc.**, 14, (1975), pp.327-340
- [7] Kang,T. et al., **NURETH-5**, (1992), pp.541-546
- [8] Keulegan,G.H., **U.S.N.B.S.Report** 5831 (1958)
- [9] Merzkirch.W., **Flow Visualization**, Academic Press (1974)
- [10] Fumizawa,M. et. al., **J. At. Energy Soc. Japan**, Vol.31, (1989), pp.1127-1128